An integrated single- and two-photon non-diffracting light-sheet microscope

Sze Cheung Lau, Hoi Chun Chiu, Luwei Zhao, Teng Zhao, M. M. T. Loy, and Shengwang Du

Citation: Review of Scientific Instruments **89**, 043701 (2018); doi: 10.1063/1.5020154
View online: https://doi.org/10.1063/1.5020154
View Table of Contents: http://aip.scitation.org/toc/rsi/89/4
Published by the American Institute of Physics

An integrated single- and two-photon non-diffracting light-sheet microscope

Sze Cheung Lau,[1] Hoi Chun Chiu,[1] Luwei Zhao,[2] Teng Zhao,[2,a)] M. M. T. Loy,[1] and Shengwang Du[1,3,b)]

[1]*Department of Physics, The Hong Kong University of Science and Technology, Clear Water Bay, Kowloon, Hong Kong, China*
[2]*Light Innovation Technology Ltd., Tseung Kwan O, Hong Kong, China*
[3]*Department of Chemical and Biological Engineering, The Hong Kong University of Science and Technology, Clear Water Bay, Kowloon, Hong Kong, China*

(Received 20 December 2017; accepted 12 March 2018; published online 2 April 2018)

We describe a fluorescence optical microscope with both single-photon and two-photon non-diffracting light-sheet excitations for large volume imaging. With a special design to accommodate two different wavelength ranges (visible: 400-700 nm and near infrared: 800-1200 nm), we combine the line-Bessel sheet (LBS, for single-photon excitation) and the scanning Bessel beam (SBB, for two-photon excitation) light sheet together in a single microscope setup. For a transparent thin sample where the scattering can be ignored, the LBS single-photon excitation is the optimal imaging solution. When the light scattering becomes significant for a deep-cell or deep-tissue imaging, we use SBB light-sheet two-photon excitation with a longer wavelength. We achieved nearly identical lateral/axial resolution of about 350/270 nm for both imagings. This integrated light-sheet microscope may have a wide application for live-cell and live-tissue three-dimensional high-speed imaging. *Published by AIP Publishing.* https://doi.org/10.1063/1.5020154

I. INTRODUCTION

Light-sheet fluorescence microscopy has been demonstrated for its strength in imaging three-dimensional (3D) live samples as it offers both faster acquisition and significantly reduced phototoxicity as compared to scanning confocal microscopy.[1–3] For achieving a high 3D imaging resolution, it is desirable to have the illumination light sheet as thin as possible and the area as large as possible.[4] However these two requirements contradict each other for the conventional Gaussian-beam based light-sheet microscopes (LSMs): As the thickness of the light sheet approaches to the diffraction limit of $\lambda/2$, the propagation length (or Rayleigh range) reduces to about one wavelength (λ) which leads to a very limited field of view. That is partly the reason why the use of Gaussian-beam LSM had been focused on large samples with axial resolution ≥ 1 μm.[1,2] A scanning Bessel beam (SBB), with its non-diffracting property, could be implemented to extend the sheet area and obtain both lateral and axial resolution approaching the diffraction limit, but its strong side lobes induce additional off-plane phototoxicity.[4] Therefore, an SBB LSM is often used as excitation for nonlinear microscopies, such as two-photon microscopy[5,6] and stimulated emission depletion microscopy.[7] For single-photon LSM, Chen *et al.* invented the lattice LSM (LLSM) in which non-diffracting light sheets are realized with two-dimensional lattice pattern structures.[8] Recently, we demonstrated a simple and robust method to create non-diffracting ultrathin line Bessel sheets (LBSs) for a single-photon LSM.[9]

It is of practical importance to have a single microscope system that can be operated in both single- and two-photon excitation modes. For single-photon excitation, the LLSM or LBS is the preferable choice, but its direct 2D sheet configuration, which spreads the light energy on a large area and results in weak intensity, is not suitable for two-photon excitation that requires a high instantaneous intensity. For a two-photon LSM, the SBB is the optimal solution. Building the LLSM/LBS and SBB together in one system remains a technical challenge because LBS and SBB have to be generated separately before combined at the back of the excitation objective due to the difference in their optical setups. The vast span in spectrum between the two modes also causes a significant misalignment between the LBS and SBB, and they must be adjusted separately in order to image the same position of a sample with both single-photon and two-photon light sheets. In this article, we demonstrated a novel setup that combines the single-photon LBS and two-photon SBB light sheets into a single microscope system. We achieved a near isotropic resolution of around 300 nm for both single- and two-photon imaging modes. In the single-photon LBS, we acquired 3D images of cells or superficial layers of tissues with ease, while the two-photon SBB can be used for imaging deep tissue or small animals like zebrafish with a higher signal to noise ratio (SNR).

II. OPTICAL SETUP

The experimental schematic of the integrated non-diffracting light-sheet microscope is shown in Fig. 1, where the single-photon LBS (488 nm, blue dashed traces) and two-photon SBB (680-1080 nm tuneable, red solid traces) light sheets are combined at a dichroic mirror (longpass cutoff at 680 nm). The optical system design takes into account the large wavelength difference and the mode compatibility. Lenses L1–L8 are all achromatic doublets designed at visible wavelengths (400-700 nm), while L9–L19 are achromatic doublets for near

a)Electronic mail: tengzhao@lit.com.hk
b)Electronic mail: dusw@ust.hk

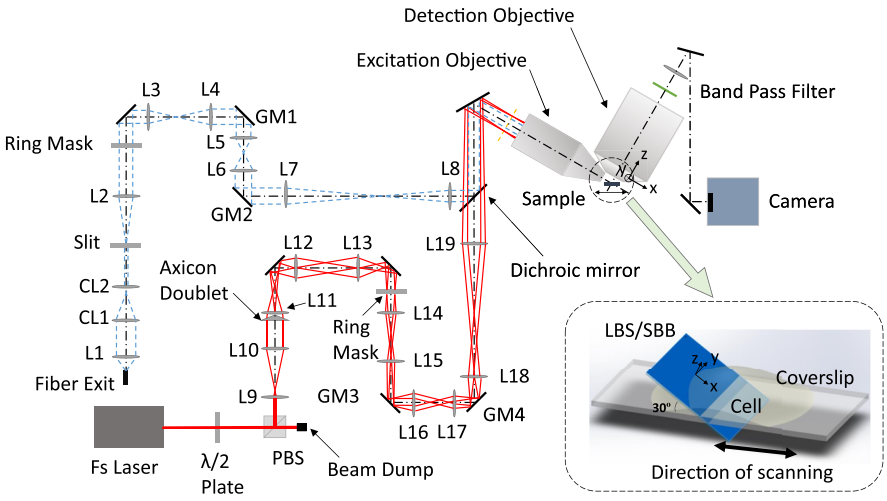

FIG. 1. Optical setup of the integrated single-photon LBS and two-photon SBB non-diffracting light-sheet microscope. Blue dashed rays: LBS single-photon light sheet (488 nm). Red solid rays: SBB two-photon light sheet (800 nm). All lenses used in the system are achromatic doublets to minimize the chromatical aberrations due to the large wavelength span. L1–L8 and CL1 and CL2 are all designed for visible light 400-700 nm while lenses L9–L19 are designed for 650-1050 nm. In the coordinate system, the x axis is along the sheet beam propagation direction, and the z direction is along the imaging optical axis.

infrared beams (650-1050 nm). The lateral positions of the LBS and SBB can be adjusted individually by galvo-mirrors GM2 and GM4. Shifting L19 along the beam axis will reposition the focused ring produced by the axicon and annulus to be overlapped with the focused pattern of the LBS at the back aperture of the excitation objective so that the axial position of the SBB and LBS can be matched perfectly at the sample. With these degrees of freedoms for adjustment, single-photon LBS and two-photon SBB can be both aligned to the focal plane of the detection objective. As shown in Fig. 1 and its inset, the xyz coordinate system is chosen as the following: the sheets are on the x-y plane with the x axis along the beam propagation direction, and the z direction is along the imaging optical axis.

A. LBS single-photon light sheet

The blue dashed rays in Fig. 1 illustrate the optical layout of the LBS single-photon light sheet. We use a diode laser (488 nm, Coherent OBIS) output as the single-photon excitation light source. After passing through an acousto-optical tunable filter (Gooch & Housego, 400-700 nm) for intensity modulation, the laser light is coupled to an optical single-mode fiber (not shown). The collimated light from the fiber exit is shaped by a pair of cylindrical lenses (CL1 and CL2) placed in parallel to compress in one direction so that the most of the light passes through a single slit with a width of 0.2 mm. The Fourier transform of the slit is then cropped by a ring mask (with inner and outer radii of 1.973 mm and 0.657 mm, respectively) to achieve the non-diffracting property. At this point, an image of two collinear and truncated lines passes through the mask. This image is conjugated with two galvo-mirrors scanning in the x (GM1) and z (GM2) directions and finally to the back focal plane of excitation objective (Light Innovation Technology Ltd, LS29 ApoPlan LWD 29 × 0.55 NA, water immersion) by pairs of relay lenses (L7-L8). The excitation objective transforms the pattern at its back focal plane to produce the final light sheet with a center thickness less than 400 nm. GM1 scans the light sheet in the focal plane of the detection objective such that a much larger field of view can be covered, and GM2 aligns the light sheet precisely to the focal plane of the detection objective. The details of the LBS are also described in Ref. 9.

B. SBB two-photon light sheet

The red solid rays in Fig. 1 illustrate the optical layout of the SBB two-photon light sheet. Here we work with a femtosecond laser (800 nm, 2.9 W, Coherent Chameleon Ultra I). A broadband half-wave plate (680-1080 nm) in the beam path is rotated to adjust the amount of laser power reflected by the polarizing beam splitter (PBS) while the rest of the energy is dumped to a heat-dissipating beam dump. The reflected laser beam is then expanded by a telescope lens pair and shaped

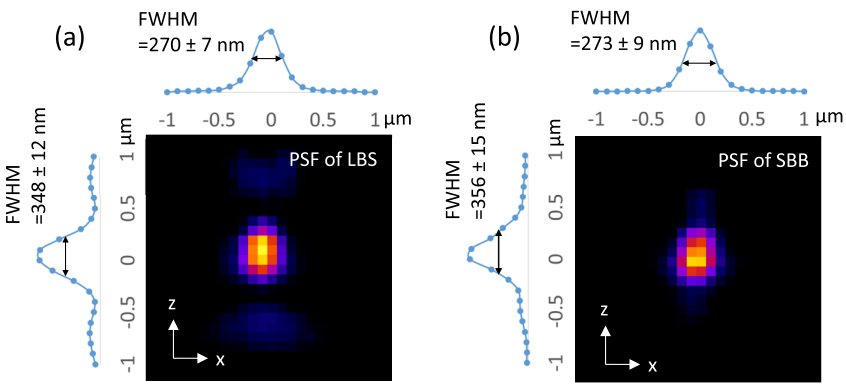

FIG. 2. Measurements of the PSFs. The y projections on the z-x plane of the 20-nm bead images for (a) LBS single-photon and (b) SBB two-photon microscopies.

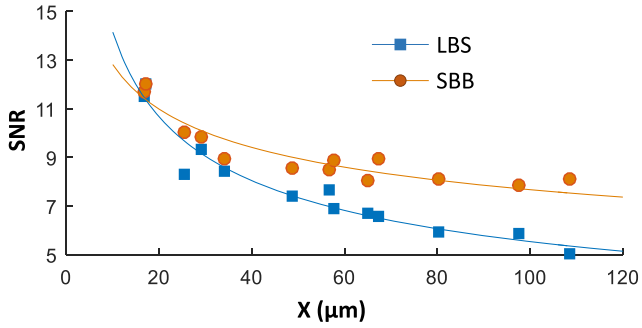

FIG. 3. SNR as a function of depth along the x-axis for LBS single-photon and SBB two-photon LSMs. The solid curves are exponential decay with best fitted decay coefficients 0.016/μm (fitting goodness by R-square: 97%) and 0.009/μm (R-square: 95%) for LBS and SBB, respectively.

by an axicon (Thorlabs, AX251-B) closely placed in front of the lens L11 to produce a ring image. This image is cropped by a ring mask (with inner and outer radii of 7.17 mm and 6.023 mm, respectively) to filter out the unwanted components produced by the imperfection of the axicon. This ring image is conjugated to another set of galvo-mirrors (GM3 and GM4) and further relayed by the lens pair L18 and L19, then finally projected to the back focal plane of excitation objective, and produce the SBB at the focus of the excitation objective which is carefully aligned to the focal plane of the detection objective and overlaps with LBS. The SBB is scanned by GM3 to form the light sheet for imaging.

C. Fluorescence imaging system

In the fluorescence imaging part, we use a high-NA detection objective (Nikon, CFI APO LWD, NA = 1.1, water immersion) which is placed 90° to the excitation objective and 60° to the sample plane. We define the z axis of the system to be along the optical axis of the detection objective, and the x axis is along that of the excitation objective. A set of band pass filters are placed after the detection objective to select the fluorescence signal. The final image is formed by a tube lens and detected by an scientific complementary metal–oxide–semiconductor (sCMOS) camera (Hamamatsu Flash 4.0 V3).

III. CHARACTERIZATION

To characterize the system performance, we use 20-nm-diameter fluorescence beads for measuring the 3D point spread functions (PSFs) of both LBS and SBB microscopies. The beads were coated on coverslip and excited by 488 nm and 800 nm laser light for the LBS and SBB, respectively. The y projections on the z-x plane of the bead images are displayed in Fig. 2. The y-direction, which is identical to the x-direction, is not shown here. The full widths at half maximum (FWHM) of the PSFs are 348 ± 12 nm (axial) and 270 ± 7 nm (lateral) in LBS single-photon microscopy and 356 ± 15 nm (axial) and 273 ± 9 nm (lateral) in SBB two-photon microscopy. Thus, we achieve nearly the same 3D resolution for both LBS single-photon and SBB two-photon images.

The advantage of the two-photon microscopy is that its longer wavelength allows longer light sheets for exciting deeper samples with reduced scattering, as compared to the single-photon microscopy. Here we define the imaging depth as the penetration depth of the light sheet from the sample surface along the x direction, as shown in the inset of Fig. 1. We compare the imaging depth of the LBS single-photon and SBB two-photon LSMs using the same sample of yeasts with a part of DNA strands labeled with green fluorescent protein (GFP) immersed in 6% agarose which is a good analogy of the structures of a thick biological tissue. The SNR at different penetration depths of both light sheets is plotted in Fig. 3. The decay coefficients for the LBS and SBB are 0.016/μm and 0.009/μm, respectively. At SNR = 7, the LBS can only go to a depth of 60 μm, but the SBB goes beyond 120 μm. This result indicates that the SBB two-photon light sheet is able to image (at the same SNR) much deeper into the yeast-agarose sample than the LBS single-photon light sheet.

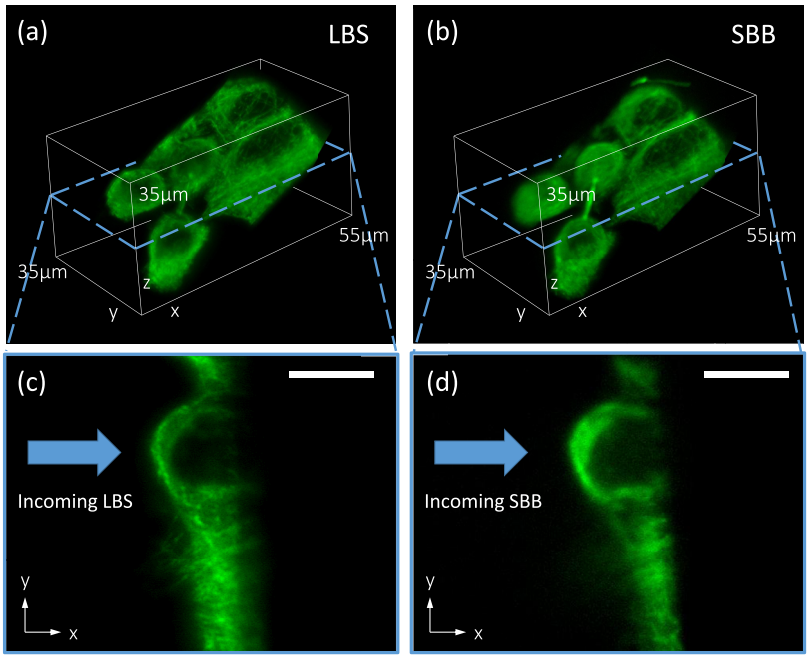

FIG. 4. Imaging a thin sample of microtubules of HT22 cells. (a) and (b) are the 3D images of cells obtained using LBS single-photon and SBB two-photon LSMs, respectively. (c) and (d) are the x-y cross-sectional views along the plane as marked by blue dashed lines in (a) and (b), respectively. Scale bars: 10 μm.

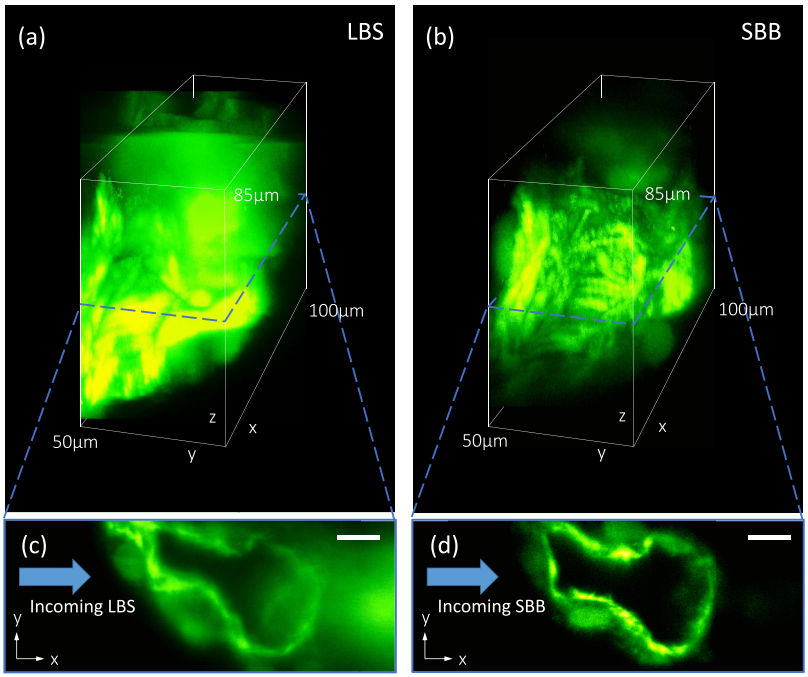

FIG. 5. Images of a GFP tagged zebrafish heart (myocardial structures) in a 48 hpf zebrafish embryo using (a) LBS single-photon and (b) SBB two-photon LSMs. (c) and (d) are the x-y cross-sectional views along the plane indicated by the blue dashed lines in (a) and (b), respectively. Scale bars: 10 μm.

IV. EXAMPLES

As an example of application, we first image Alexa488 tagged microtubules in fixed HT22 cells cultured on a coverslip to show the capability of both LBS and SBB light sheets in thin samples, as shown in Fig. 4. The cells form a monolayer on the surface of a coverslip, and the depth between the top of the cell body to the coverslip is 10 ± 2 μm along the x-axis. For this thin sample, both single-photon and two-photon light sheets imaging provide nearly the same SNR (SNR = 17.3 ± 1.2 for LBS and SNR = 16.5 ± 1 for SBB). Here the laser light power for LBS is 20 μW, while for SBB is 300 mW. Therefore, the LBS single-photon LSM is the optimal solution for imaging thin samples with much weaker excitation laser power.

To explore the performance of LBS and SBB in deep tissue imaging, we image the GFP tagged zebrafish heart (myocardial structures) in a 48 hpf zebrafish embryo. Figure 5 shows the 3D images and the x-y plane cross sections of the myocardial structures up to 100 μm deep beneath the surface of the embryo, taken by the LBS single-photon and SBB two-photon LSM, respectively. In these scattering thick samples, the LBS single-photon LSM suffers significantly greater background and much reduced SNR in comparison to the SBB two-photon LSM. In the SBB technique, its longer excitation wavelength reduces the scattering and thus maintains the shape of light sheet for a longer propagation distance than that in the LBS. Meanwhile, the scattered laser light becomes too weak to excite fluorophores that are outside the light sheet. As a result, the out-of-sheet background noise is also significantly reduced in the two-photon LSM.

V. SUMMARY AND DISCUSSION

In summary, we have developed a LSM integrated with both LBS single-photon and SBB two-photon excitations. For imaging thin samples, both LBS and SBB give nearly an identical 3D axial/lateral resolution of about 350 nm/270 nm and high SNR, but the LBS is the preferred solution because of its much lower laser power requirement and easier maintenance, as confirmed by imaging microtubules of HT22 cells. For thick samples with significant single-photon scattering, the SBB two-photon LSM provides much better imaging quality, as shown in the zebrafish embryo heart images.

Although in this paper we demonstrate the capability of the system using single wavelength LBS at 488 nm, multiple laser lines can be intergraded into the system for multi-color single photon florescent imaging. It is worthwhile to mention that, because of the wider application of single-photon fluorescence imaging, various good single-photon fluorophores are readily available with known spectra and other properties, but this is not the case in two-photon excitation. Efficient single-photon fluorophores are not always suitable for two-photon excitation. To image samples in two-photon with high contrast, more research is needed to be conducted to find the best fluorophore and most suitable wavelength. To obtain the same contrast, two-photon laser power needs to be tens of thousands or hundreds of thousands stronger than single-photon laser power. In this high-power setting, photobleaching becomes serious, and even the heating effect could cause damage or degradation on the sample. In this sense, our developed microscope not only extends the capacity of an LSM but also provides a testing platform for two-photon fluorophores which can be compared directly with its single-photon excitation of the same imaging area in the same setup.

ACKNOWLEDGMENTS

The work was supported by a grant from the Offices of the Provost, VPRG and Dean of Science, the Hong Kong University of Science and Technology (HKUST, Project No. VPRGO12SC02), and the Hong Kong Research Grants

Council (Project No. C6030-14E). S.D. acknowledges support from Light Innovation Technology Ltd through a research contract with HKUST R and D Corporation Ltd (Project Code 16171510). S.C.L. and H.C.C. acknowledge the Undergraduate Research Opportunities Program at HKUST. We thank Aifang Cheng and Claire Shuk-Kwan Lee at Division of Life Science, HKUST for providing the biological specimens.

[1]K. Greger, J. Swoger, and E. H. K. Stelzer, "Basic building units and properties of a fluorescence single plane illumination microscope," Rev. Sci. Instrum. **78**, 023705 (2007).

[2]P. J. Keller, A. D. Schmidt, J. Wittbrodt, and E. H. K. Stelzer, "Reconstruction of zebrafish early embryonic development by scanned light sheet microscopy," Science **322**, 1065 (2008).

[3]P. A. Santi, "Light sheet fluorescence microscopy: A review," J. Histochem. Cytochem. **59**, 129–138 (2011).

[4]L. Gao, L. Shao, B.-C. Chen, and E. Betzig, "3D live fluorescence imaging of cellular dynamics using Bessel beam plane illumination microscopy," Nat. Protoc. **9**, 1083 (2014).

[5]T. A. Planchon, L. Gao, D. E. Milkie, M. W. Davidson, J. A. Galbraith, C. G. Galbraith, and E. Betzig, "Rapid three-dimensional isotropic imaging of living cells using Bessel beam plane illumination," Nat. Methods **8**, 417 (2011).

[6]F. O. Fahrbach, V. Gurchenkov, K. Alessandri, P. Nassoy, and A. Rohrbach, "Light-sheet microscopy in thick media using scanned Bessel beams and two-photon fluorescence excitation," Opt. Express **21**, 13824 (2013).

[7]P. Zhang, P. M. Goodwin, and J. H. Werner, "Fast, super resolution imaging via Bessel-beam stimulated emission depletion microscopy," Opt. Express **22**, 12398 (2014).

[8]B. C. Chen, W. R. Legant, K. Wang, L. Shao, D. E. Milkie, E. Daniel, M. W. Davidson, W. Michael, C. Janetopoulos, X. S. Wu, J. A. Hammer, Z. Liu, B. P. English, Y. Mimori-Kiyosue, D. P. Romero, A. T. Ritter, J. Lippincott-Schwartz, L. Fritz-Laylin, R. D. Mullins, D. M. Mitchell, J. N. Bembenek, A. C. Reymann, R. Böhme, S. W. Grill, J. T. Wang, G. Seydoux, U. S. Tulu, D. P. Kiehart, and E. Betzig, "Lattice light-sheet microscopy: Imaging molecules to embryos at high spatiotemporal resolution," Science **346**, 1257998 (2014).

[9]T. Zhao, S. C. Lau, Y. Wang, Y. Su, H. Wang, A. Cheng, K. Herrup, N. Y. Ip, S. Du, and M. M. T. Loy, "Multicolor 4D fluorescence microscopy using ultrathin Bessel light sheets," Sci. Rep. **6**, 26159 (2016).